Pulsar timing array analysis for black hole backgrounds

Neil J Cornish[1] **and A Sesana**[2]

[1] Department of Physics, Montana State University, Bozeman, MT 59717, USA
[2] Max Planck Institut fr Gravitationsphysik (Albert-Einstein-Institut), D-14476 Potsdam, Germany

E-mail: cornish@physics.montana.edu

Abstract

An astrophysical population of supermassive black hole binaries is thought to be the strongest source of gravitational waves in the frequency range covered by pulsar timing arrays (PTAs). A potential cause for concern is that the standard cross-correlation method used in PTA data analysis assumes that the signals are isotropically distributed and Gaussian random, while the signals from a black hole population are likely to be anisotropic and deterministic. Here we show that while the conventional analysis is not optimal for detecting signals from black hole binaries, the technique still works as the standard Hellings–Downs correlation curve turns out to hold for point sources. Moreover, the small effective number of signal samples blurs the distinction between Gaussian and deterministic signals. Possible improvements to the standard cross-correlation analysis that account for the anisotropy of the signal are discussed.

PACS numbers: 95.85.Sz, 04.25.dg, 97.60.Gb

(Some figures may appear in colour only in the online journal)

1. Introduction

The most promising source of signals in the frequency range covered by pulsar timing arrays (PTAs) is from a population of supermassive black hole (BH) binaries, dominated by systems with masses in the range $3 \times 10^7 M_\odot$ $3 \times 10^9 M_\odot$, and times to merger in the range 10^3 years 10^5 years. It had been assumed that the number density of sources as a function of frequency, dN/df, would be sufficiently large that the central limit theorem would come into play, and that the combined signal would be Gaussian distributed and isotropic. However, recent studies based on more realistic population synthesis models have shown that the signal is likely to be dominated by a small number of relatively nearby sources [1–4], and as a result, will be non-Gaussian and anisotropic [5, 6]. This is a concern since the standard analysis techniques [7–9] are based on the assumption that the signal is isotropic and Gaussian.

Here we show that, while the standard approach may not be optimal, it is able to detect the signals from isolated BHs, and by extension, populations of BHs no matter how sparse. What makes this possible is the rather surprising result that the Hellings–Downs correlation curve [7], which was originally derived for un-polarized, isotropic backgrounds, continues to be valid for polarized point sources! Like many results that are surprising initially, after a little thought this result starts to make sense (it is basically a reflection of the quadrupole nature of the signal), and very soon the result becomes obvious, and soon after that, something everyone knew already.

While the standard cross-correlation analysis technique can be used to detect the signals from a sparse BH background, it will not be optimal. We consider a variety of alternative analysis techniques that may be more effective, and suggest a new cross-correlation technique that accounts for the anisotropy of the signal.

2. Detector response

The timing residuals for a pulsar located in the $\hat{n}$ θ_p, ϕ_p) direction, induced by a plane gravitational wave from a source in the θ, ϕ) direction, can be expressed as

$$r = \tfrac{1}{2} R_+ \cos 2\psi F^+ - \sin 2\psi F^\times) + R_\times \sin 2\psi F^+ + \cos 2\psi F^\times)), \qquad (1)$$

where ψ is the polarization angle of the wave relative to the frame defined by the basis vectors $\hat{u}, \hat{v}$ that span the plane perpendicular to the propagation direction $\hat{k}$, where

$$\hat{k} = - \sin\theta \cos\phi \, \hat{x} + \sin\theta \sin\phi \, \hat{y} + \cos\theta \, \hat{z}),$$
$$\hat{u} = \cos\theta \cos\phi \, \hat{x} + \cos\theta \sin\phi \, \hat{y} - \sin\theta \, \hat{z}, \qquad (2)$$
$$\hat{v} = \sin\phi \, \hat{x} - \cos\phi \, \hat{y}.$$

The antenna beam pattern functions have the form

$$F^+ = \frac{\hat{u} \cdot \hat{n})^2 - \hat{v} \cdot \hat{n})^2}{1 + \hat{k} \cdot \hat{n}}$$
$$F^\times = \frac{2 \, \hat{u} \cdot \hat{n}) \, \hat{v} \cdot \hat{n})}{1 + \hat{k} \cdot \hat{n}}. \qquad (3)$$

The terms $R_{+,\times}$ are expressed in terms of the anti-derivative, $H_{+,\times}$ of the gravitational wave strain $h_{+,\times}$:

$$R_{+,\times} = H_{+,\times} \, t) - H_{+,\times} \, t - L \, 1 + \hat{k} \cdot \hat{n})), \qquad (4)$$

where L is the distance to the pulsar from Earth. The two terms in the above equation are referred to as the 'Earth term' and the 'pulsar term', respectively. For nearby sources the plane wave approximation may need to be augmented by the leading order spherical wavefront corrections of order L/D, where D is the distance to the source:

$$R_{+,\times} = H_{+,\times} \, t) - H_{+,\times} \, t - L \, 1 + \hat{k} \cdot \hat{n}) + \frac{L^2}{D} \, 1 - \hat{k} \cdot \hat{n})^2)). \qquad (5)$$

The antenna patterns can be re-written in the alternative, simpler form

$$F^+ = 1 + \cos\beta) \cos 2\alpha)$$
$$F^\times = 1 + \cos\beta) \sin 2\alpha), \qquad (6)$$

where $\beta = \arccos -\hat{k} \cdot n)$ is the angle between the source and the pulsar, and $\alpha = \arctan \hat{v} \cdot \hat{n})/ \hat{u} \cdot \hat{n}))$ is the angle the pulsar direction makes relative to the $\hat{u}, \hat{v}$ polarization frame. The timing residuals then take the form

$$r = \tfrac{1}{2} R_+ \cos 2\psi + 2\alpha) + R_\times \sin 2\psi + 2\alpha)) \, 1 + \cos\beta). \qquad (7)$$

3. Correlation analysis

The cross-correlation of the timing residuals from two pulsars can be written as

$$\langle r_i r_j \rangle = \tfrac{1}{4} \left(\langle R_+^2 \rangle \cos(2\psi + 2\alpha_i) \cos(2\psi + 2\alpha_j) \right.$$
$$\left. + \langle R_\times^2 \rangle \sin(2\psi + 2\alpha_i) \sin(2\psi + 2\alpha_j) \right) (1 + \cos\beta_i)(1 + \cos\beta_j), \tag{8}$$

where the angle brackets denote the inner product

$$\langle h_1 h_2 \rangle = \int dt_1 \int dt_2 \, h_1(t_1) K(t_1, t_2) h_2(t_2). \tag{9}$$

For stationary signals, the convolution kernel is a function of the lag $|t_1 - t_2|$, and the inner product can be re-written in the Fourier domain in the familiar form

$$\langle h_1 h_2 \rangle = \int_0^\infty \frac{2(\tilde{h}_1(f) \tilde{h}_2^*(f) + \tilde{h}_1^*(f) \tilde{h}_2(f))}{S(f)} \, df. \tag{10}$$

In (8) it has been assumed that $\langle R_+ R_\times \rangle = 0$, which holds for cosmological stochastic backgrounds and binary systems. For isotropic gravitational wave backgrounds it makes sense to average the cross-correlation over the sky:

$$\frac{1}{4\pi} \int \langle r_i r_j \rangle \, d\Omega = \langle H^2 \rangle \, \alpha_{ij}, \tag{11}$$

where $\langle H^2 \rangle = \langle R_+^2 + R_\times^2 \rangle$, and the Hellings–Downs correlation curve $\alpha_{ij} = \alpha(\theta_{ij})$ is given as a function of the angle $\theta_{ij} = \mu$ between the pulsars:

$$\alpha(\mu) = \frac{1 - \cos\mu}{2} \ln\left(\frac{1 - \cos\mu}{2} \right) - \frac{1 - \cos\mu}{12} + \frac{1}{3}(1 + \delta(\mu)). \tag{12}$$

The delta function—defined such that $\delta(0) = 1$, and is otherwise zero—comes from the pulsar term, which averages to a non-zero value in the auto-correlation.

For anisotropic signals, such as those produced by a single BH binary, sky averaging is not justified, and the correlation $\langle r_i r_j \rangle$ will depend on the sky location of the source (θ, ϕ), and the orbital orientation given in terms of the inclination and polarization angles (ι, ψ). It had been assumed that an astrophysical population of binaries would combine to yield an isotropic, stochastic background, but this turns out not be the case. Instead the combined signal is dominated by a handful of nearby, bright sources, and as shown in figure 1, the resulting background is highly anisotropic. The BH population model used to generate figure 1 was derived by extracting catalogues of merging massive galaxies from the Bertone *et al* [10] semianalytic model built on top of the Millennium Run [11]. Galaxies were then populated with supermassive BHs correlating with the bulge velocity dispersion as given by Gultekin *et al* [12]. The BHs accrete gas prior to final coalescence and all binaries are assumed to be circular and driven by GW emission only in the frequency band relevant to PTA. All the steps of the procedure followed to construct the population are given in [2]. The anisotropy seen in figure 1 is even more pronounced if the signal is broken out by frequency bins, where a single source often dominates in a particular bin. The question then becomes, what is the best technique to detect such a signal, given that it is neither isotropic nor Gaussian? These assumptions underpin the standard analysis techniques in both the frequentist and Bayesian implementations. The frequentist approach is based on the matched filter detection statistic [8]

$$\rho = \sum_i \sum_{j \neq i} \langle r_i r_j \rangle \alpha(\theta_{ij}). \tag{13}$$

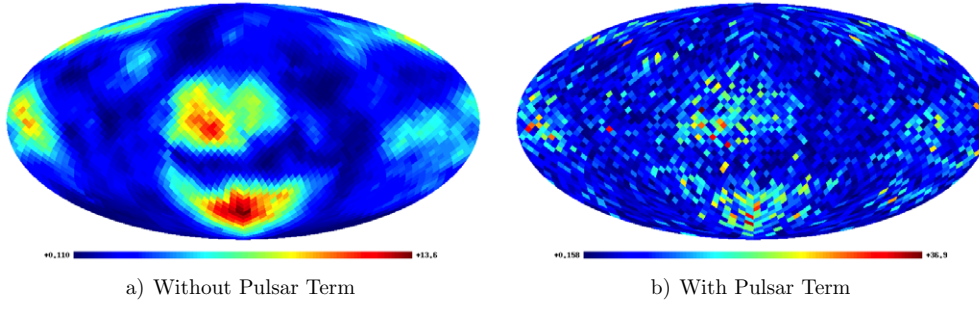a) Without Pulsar Term　　　　　　　　　　b) With Pulsar Term

Figure 1. The auto-correlated signal power $\langle r^2 \; \theta_p, \phi_p)\rangle$ for a single realization of a BH binary population model. The linear color scale is in arbitrary units. The left panel has the 'pulsar terms' turned off, while the right panel shows the full response. The pulsar term adds noise, effectively multiplying the Earth-term sky map by $2 \; 1 - \cos \; \delta))$, where δ is a random phase. Generating the full response at higher angular resolution and then applying a Gaussian smoothing yields a sky map nearly identical to the map with the pulsar term turned off. Either way, the anisotropy of the signal is clear, with pulsars in certain sky directions receiving significantly larger signal power than others.

This statistic is often shifted to have zero mean and scaled to have variance $1/N_{\text{pairs}}$, where $N_{\text{pairs}} = N \; N - 1)/2$ are the number of pulsar pairs. The key idea is that the pairwise correlations are summed together after being multiplied by the expected correlation function, which acts like a matched filter. In the Bayesian approach, the correlation function enters into the definition of the multi-variate Gaussian likelihood function [9, 13, 14],

$$p = A \exp\left(- \sum_{i,j} \int \; \tilde{r}_i \tilde{r}_j^* + \tilde{r}_i^* \tilde{r}_j) C_{ij}^{-1} \, df - \frac{1}{2} \int \ln \; \det C) \, df \right),　　　(14)$$

where A is an overall normalization constant and

$$C_{ij} \; f) = S_H \; f) \alpha_{ij} + S_{n_i} \; f) \delta_{ij}.　　　(15)$$

Here $S_H \; f)$ is the power spectral density of the signal and $S_{n_i} \; f)$ is the power spectral density of the noise in the ith pulsar. In the weak-signal limit, $S_{n_i} \gg S_H$, the likelihood (14) can be approximated as $p = A' \exp \; \rho/2)$, drawing out the close connection between the two approaches.

4. Isolated black hole binaries

Before discussing alternative analysis techniques that may be better suited to detecting anisotropic, non-Gaussian signals, it is interesting to consider how the standard analysis might perform at detecting the signal from an isolated BH binary. To set the stage, let us consider the correlations produced in a PTA with 100 randomly distributed pulsars by (i) a single BH binary; and (ii) an isotropic background. To make the comparison equitable, the isotropic signal was restricted to a single frequency bin. In figure 2 the correlations are shown both with and without the pulsar term, and un-binned and binned in the angular separation between the pulsars. The signal strength in each case was scaled to give unit correlation at $0°$ separation. The results in both cases are very similar. The un-binned correlations show significant scatter, while the binned correlations follow the Hellings–Downs correlation curve. At first sight it may seem strange that an isolated BH binary produces a correlation pattern
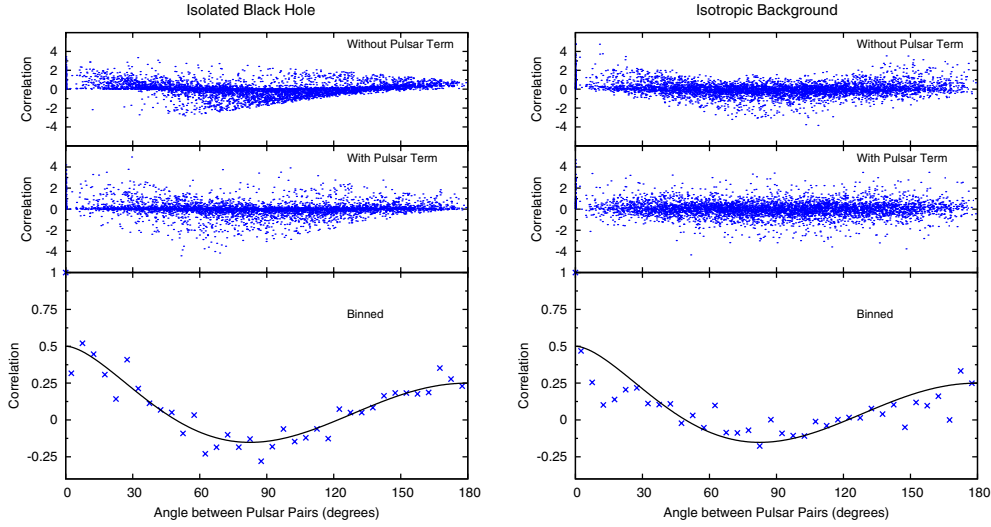
Figure 2. Simulated noise free correlation curves for (i) an isolated BH binary (ii) an isotropic background restricted to a single frequency bin. The top panels show the correlations as a function of the angle between the pulsar pairs without the 'pulsar term'; the middle panels show the full correlation; while the lower panels show the full correlations averaged into 5° bins. The correlations have been scaled such that the average of the auto-correlation terms is unity.

that is identical to that produced by an isotropic background, but on reflection the result is not surprising. The Hellings–Downs curve is simply a consequence of the quadrupolar nature of gravitational waves. In binning the correlations as a function of the pulsar angular separation we are replacing the sky average (11) by an average over the pulsar locations, which in the limit of a large number of pulsar pairs goes over to the integral

$$\gamma(\mu) = \frac{1}{(4\pi)^2} \int \langle r_i r_j \rangle \, \delta(\cos \mu - \hat{n}_i \cdot \hat{n}_j) \, d\Omega_i \, d\Omega_j. \tag{16}$$

The Dirac-delta function can be taken care of by adopting a coordinate system where the j-pulsar has coordinates

$$\begin{aligned}
x_j &= \cos \phi_i \, (\cos \theta_i \sin \mu \cos \lambda + \sin \theta_i \cos \mu) - \sin \phi_i \sin \mu \sin \lambda \\
y_j &= \sin \phi_i \, (\cos \theta_i \sin \mu \cos \lambda + \sin \theta_i \cos \mu) + \cos \phi_i \sin \mu \sin \lambda \\
z_j &= \cos \theta_i \cos \mu - \sin \theta_i \sin \mu \cos \lambda,
\end{aligned} \tag{17}$$

which ensure that $\hat{n}_i \cdot \hat{n}_j = \cos \mu$. Completing the integration over λ, ϕ_i, θ_i yields

$$\gamma(\mu) = \langle H^2 \rangle \alpha(\mu). \tag{18}$$

Thus, a single BH produces an identical angular correlation pattern as an isotropic stochastic background. Note that the final result is independent of the BH orientation or sky position. Again, this is not surprising since we have integrated the pulsar locations over the celestial sphere, which is equivalent to actively rotating the BH reference frame while holding the pulsars locations fixed.

The simulations in figure 2 used 100 pulsars so that the correlation pattern would be obvious by eye after binning, however, the correlation is detectable with far fewer pulsars. Figure 3 shows Bayes factors (betting odds) for the correlations following the Hellings–Downs curve versus there being no correlation (aside from the auto-correlation of a pulsar with itself).
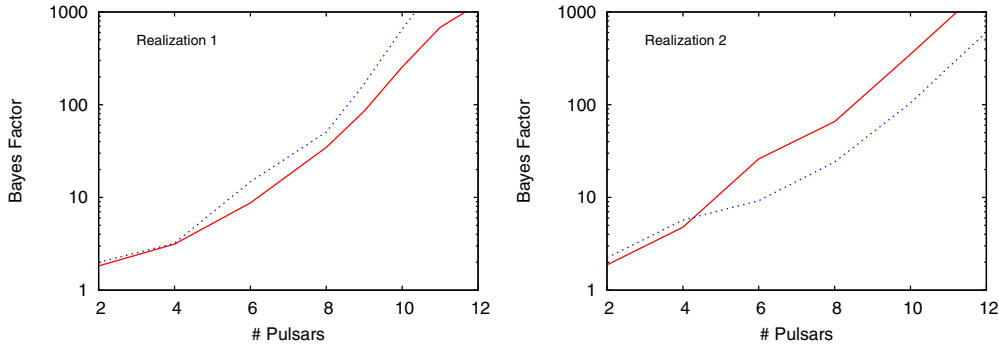
Figure 3. Bayes factors for the detectability of the Hellings–Downs correlation as a function of the number of pulsars in the array for two realizations of simulated data. In each panel the solid (red) line is for an isotropic background restricted to a single frequency bin, while the dotted (blue) line is for an isolated BH binary. The pulsar term was set to zero. There are fluctuations between realizations, but on average, the correlations induced by a single BH are just as detectable as for an isotropic background.

The correlation pattern becomes detectable with ∼8 or more pulsars. This is true both for an isotropic background and for a single BH binary. Note that the Bayes factors do not change if we rescale the correlation data by an overall constant.

5. Astrophysical black hole populations

In [6] the applicability of the standard analysis techniques based on (13) and (14) for detecting the signals from an astrophysical population of BHs was discussed. There the focus was on the non-Gaussianity of the signal, rather than the anisotropy. It was noted that the correlations between pulsars followed the Hellings–Downs correlation curve upon averaging over ∼100 realizations (unsurprising given that the averaging restores isotropy), but this result has little practical relevance given that we only get to see a single realization. On the other hand, the fact that a *single* BH binary yields the Hellings–Downs curve means that the standard analysis techniques will be effective (though not necessarily optimal) at detecting the signal from a population of BHs. And while it is possible to theoretically establish the non-Gaussianity of the signal using hundreds of realizations of the population catalogs, it will be difficult to establish in practice with the handful of frequency bins available for the analysis. Indeed, the departure from Gaussianity will likely be established by the detection of one or more of the brightest signals using single source analysis techniques [15, 16]. The importance of there being few effective samples in the data is illustrated in figure 4, where correlation curves for various simulated signals are shown based on a ten year observation period. Noise was not added to the signals in figure 4 so as not to obscure the intrinsic scatter from the pulsar term, but a noise spectrum was used when computing the inner products in the pulsar correlations coefficients

$$R_{ij} = \int \frac{\tilde{r}_i \tilde{r}_j^* + \tilde{r}_i^* \tilde{r}_j)}{S_n \; f)} \mathrm{d}f. \tag{19}$$

The pulsar timing noise was assumed to have a white spectrum above ∼6 nHz, and a red spectrum at lower frequencies [17]:

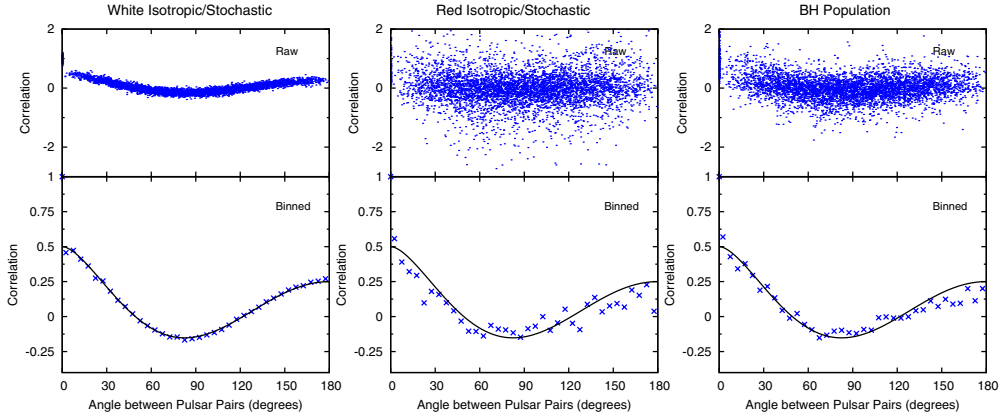$$S_n \; f) = \text{const.} \; 1 + \; f/6\,\text{nHz})^{-2}). \tag{20}$$

Figure 4. Simulated noise free correlation curves for (i) an isotropic, white Gaussian background using 100 frequency bins (ii) an isotropic red Gaussian background with the spectrum predicted for a BH population (iii) a BH population model. The upper panels are raw scatter plots as a function of the angle between the pulsars, while the lower panels average the correlations into $5°$ bins. The correlations have been scaled such that the average of the auto-correlation terms is unity.
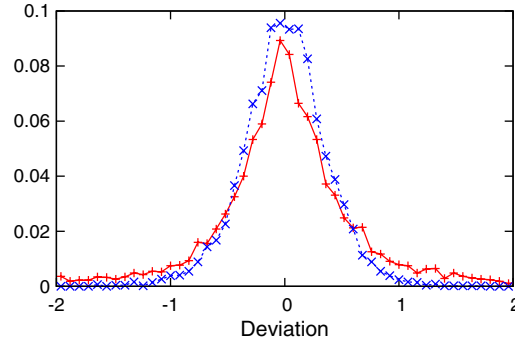

Figure 5. Histograms of the scatter in the correlation about the Hellings–Downs model for an isotropic, red Gaussian background (red, solid line), and for an astrophysical population of BH binaries (blue, dashed line).

This noise weighting in the inner product means that for the signals with very red spectra, such as those shown in the second two panels of figure 4, the correlations are dominated by the data in the first few frequency bins. The constant in (20) is irrelevant since we scale the correlations such that the average autocorrelation equals unity: $\langle R_{ii} \rangle = 1$.

The first panel in figure 4 shows the correlation curve for an isotropic stochastic background with a white spectrum that covers 100 frequency bins. The second panel shows the correlation curve for an isotropic stochastic background with a red spectrum where the slope was chosen to match that from a population of BH binaries ($S_H\ f) \sim f^{-13/3}$). The third panel shows the correlation curve for a realization of the BH population model used to generate figure 1. Remarkably, the scatter from the BH population is *less* than for an Gaussian stochastic background, as can be seen in the histograms of $R_{ij} - \frac{3}{2}\alpha\ \theta_{ij}$) shown in figure 5.

Having established that the standard correlation analysis is capable of detecting the anisotropic, deterministic signal from an astrophysical population of BH binaries, it is worth

considering how the analysis can be improved. What we are seeking is an analysis technique that has an optimal balance between fidelity in the signal model and parsimony in terms of dimensionality. High dimensional models can achieve high fidelity, but at the cost of a larger trials factor (in a frequentist setting) or Occam factor (in a Bayesian setting). One high fidelity approach would be to abandon a correlation analysis in favor of a direct waveform template-based search for individual systems [15, 16], along the lines of what has been proposed for detecting galactic binaries with a space based gravitational wave detector [18]. The advantage of such an approach is that the signal model would accurately reflect the signals in the data, but the downside is that it greatly increases the size of the parameter space to be explored. We may find ourselves in a regime where each individual source lies below the detection threshold, while the combined signal may be detectable by some other less direct approach. A correlation analysis using a variant of (8), evaluated for several bright binaries with particular orientations and sky location, and with the frequency domain inner products restricted to sub-bands where one or two signals dominate, may be effective, but such an analysis introduces almost as many parameters as a multi-signal template-based approach. One model that may find the sweet spot in the balance between fidelity and complexity introduces just a single orientation parameter for each bright source, which helps account for the anisotropy of the underlying signal. The orientation parameter is the angle ζ between the unknown source direction θ, ϕ) and the 'filter direction' θ_T, ϕ_T). In practice it is simplest to parameterize the search using the filter parameters θ_T, ϕ_T), but the physical parameter space remains one dimensional since each value of ζ corresponds to a circle on the θ_T, ϕ_T) search sphere. An analysis parameterized by the angles θ_T, ϕ_T) favors circles with large ζ, and if a uniform prior on ζ is desired a Jacobian factor of $1/\sin \zeta$ has to be included in the posterior density. To see how this model is derived, consider the filtered correlation function

$$\kappa_{ij} \theta, \phi, \theta_T, \phi_T) = \langle r_i r_j \rangle \theta, \phi) \beta_{ij} \theta_T, \phi_T), \tag{21}$$

with

$$\beta_{ij} \theta_T, \phi_T) = F_i^+ \theta_T, \phi_T) F_j^+ \theta_T, \phi_T) + F_i^\times \theta_T, \phi_T) F_j^\times \theta_T, \phi_T). \tag{22}$$

The filter $\beta_{ij} \theta_T, \phi_T)$ is the polarization averaged correlation function for a point source at sky location θ_T, ϕ_T). Note that sky average of this quantity is the standard Hellings–Downs correlation curve:

$$\frac{1}{4\pi} \int \beta_{ij} \theta_T, \phi_T) \, d\Omega_T = \alpha \theta_{ij}). \tag{23}$$

Averaging κ_{ij} over pulsar pairs separated by angle μ yields

$$\frac{1}{4\pi)^2} \int \kappa_{ij} \theta, \phi, \theta_T, \phi_T) \delta \cos \mu - \hat{n}_i \cdot \hat{n}_j) \, d\Omega_i \, d\Omega_j = \langle H^2 \rangle \gamma \mu, \zeta). \tag{24}$$

In the continuum limit, the standard ρ statistic is recovered by integrating the above expression over the pulsar separation angles μ and the orientation parameter ζ: $\rho = \int \langle H^2 \rangle \gamma \mu, \zeta) \, d\cos \mu \, d\cos \zeta$. The function $\gamma \mu, \zeta)$ is plotted in figure 6. Note that the matched filter $\gamma \mu, 0)$ produces the largest correlation, and that using the sky averaged version of the filter (i.e. the average over ζ) will degrade the sensitivity.

For a BH population the analysis could target the brightest BHs in each frequency band. For example, in the Bayesian formulation the correlation function to be used in the likelihood (14) could be generalized to

$$C_{ij} f) = \sum_k S_H^k f) \beta_{ij} \left(\theta_T^k, \phi_T^k \right) + S_{n_i} f) \delta_{ij}, \tag{25}$$

where the $S_H^k f)$ are localized to a particular frequency band. The optimal number of bands and their placement could be determined from the data using transdimensional Markov chain Monte Carlo techniques.
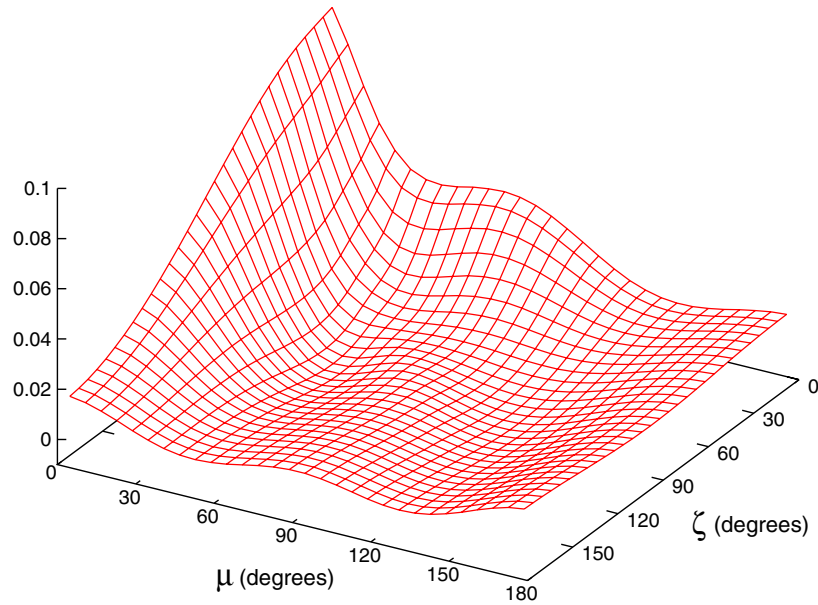
Figure 6. The directional correlation function γ μ, ζ).

6. Conclusions

We have shown that the standard cross-correlation analysis that was originally developed for isotropic, Gaussian backgrounds is capable of detecting the signals from individual black hole binaries, and by extension, the combined signal generated by an astrophysical population of binaries. We have also argued that the standard analysis will be sub-optimal in this case since the assumptions it makes about the signal are not valid, and we have suggested a number of approaches that may be more sensitive. We are currently exploring the relative performance of the various methods using simulated data from a variety of population synthesis models, and the results will be presented in a forthcoming publication.

Acknowledgment

References

[1] Sesana A, Vecchio A and Colacino C N 2008 *Mon. Not. R. Astron. Soc.* **390** 192 (arXiv:0804.4476 [astro-ph])
[2] Sesana A, Vecchio A and Volonteri M 2009 *Mon. Not. R. Astron. Soc.* **394** 2255 (arXiv:0809.3412 [astro-ph])
[3] Sesana A and Vecchio A 2010 *Class. Quantum Grav.* **27** 084016 (arXiv:1001.3161 [astro-ph.CO])
[4] Kocsis B and Sesana A 2011 *Mon. Not. R. Astron. Soc.* **411** 1467 (arXiv:1002.0584 [astro-ph.CO])
[5] Cornish N J and Sesana A 2012 *APS April Meeting Abstract* abstract no. Q7005C (http://adsabs.harvard.edu/abs/2012APS..APR.Q7005C)
[6] Ravi V, Wyithe J S B, Hobbs G, Shannon R M, Manchester R N, Yardley D R B and Keith M J 2012 *Astrophys. J.* **761** 84 (arXiv:1210.3854 [astro-ph.CO])
[7] Hellings R W and Downs G S 1983 *Astrophys. J.* **265** L39
[8] Jenet F A, Hobbs G B, Lee K J and Manchester R N 2005 *Astrophys. J.* **625** L123 (arXiv:astro-ph/0504458)

  [9] van Haasteren R, Levin Y, McDonald P and Lu T 2009 *Mon. Not. R. Astron. Soc.* **395** 1005 (arXiv:0809.0791
       [astro-ph])
 [10] Bertone S, De Lucia G and Thomas P A 2007 *Mon. Not. R. Astron. Soc.* **379** 1143 (arXiv:astro-ph/0701407)
 [11] Springel V *et al* 2005 *Nature* **435** 629 (arXiv:astro-ph/0504097)
 [12] Gultekin K *et al* 2009 *Astrophys. J.* **698** 198 (arXiv:0903.4897 [astro-ph.GA])
 [13] Finn L S 1998 *eConf* C **9808031** 07 (arXiv:gr-qc/9903107)
 [14] Cornish N J and Romano J D 2013 *Phys. Rev.* D **87** 122003 (arXiv:1305.2934 [gr-qc])
 [15] Corbin V and Cornish N J 2010 arXiv:1008.1782 [astro-ph.HE]
 [16] Ellis J A, Siemens X and Creighton J D E 2012 *Astrophys. J.* **756** 175 (arXiv:1204.4218 [astro-ph.IM])
 [17] Finn L S and Lommen A N 2010 *Astrophys. J.* **718** 1400 (arXiv:1004.3499 [astro-ph.IM])
 [18] Crowder J and Cornish N 2007 *Phys. Rev.* D **75** 043008 (arXiv:astro-ph/0611546)